



# OPEN Enhanced auditory responses in visual cortex of blind rats using intrinsic optical signal imaging

Shu Maruoka<sup>1,5</sup>, Eriko Sugano<sup>1,5</sup>, Ryunosuke Togawa<sup>2</sup>, Norihiro Katayama<sup>3</sup>, Kitako Tabata<sup>1</sup>, Naoto Yoshizawa<sup>1</sup>, Ryohei Morita<sup>1</sup>, Yuya Takita<sup>1</sup>, Taku Ozaki<sup>4</sup>, Tomokazu Fukuda<sup>4</sup>, Lanlan Bai<sup>4</sup> & Hiroshi Tomita<sup>1</sup>✉

Functional maturation of the visual cortex is induced by visual experiences during critical periods. Blind animals and humans exhibit improved auditory abilities after losing their vision. Here we investigated the response of the visual cortex to white noise stimuli during the progression of photoreceptor degeneration in a rat model of blindness (Royal College of Surgeons [RCS] (*rdy/rdy*) rats). Optical coherence tomography of RCS (+/+) rats with normal visual function revealed normal photoreceptor cells, whereas 3-month-old RCS (*rdy/rdy*) rats demonstrated photoreceptor cell degeneration. Visual cortex responses (VCRs) to a single flash stimulus were negligible in 3-month-old photoreceptor-degenerated rats. However, VCRs with white noise stimuli were significantly increased in blind versus RCS rats (+/+). Slight changes in the intrinsic optical signals of the control rats were observed on the ventral side of the visual cortex. In contrast, responses were markedly increased throughout the visual cortex of RCS (*rdy/rdy*) rats. These results indicate that the visual cortex rapidly acquires auditory system function over the first 3 months of life and that the entire visual cortex, rather than just the portion close to the auditory cortex, responds to white noise.

**Keywords** Visual cortex, Intrinsic optical signal imaging, Blindness, Auditory response, Visual evoked potential

Brain plasticity refers to synaptic restructuring in which infrequently used synapses are degraded and frequently used synapses are enhanced. There is a critical but temporary period in which brain plasticity increases; thereafter, brain function is less likely to change<sup>1</sup>. In the visual system, as neural circuits develop during the critical period, visual acuity becomes comparable to that of adults and stereopsis becomes possible. If a child receives insufficient visual input during this critical period, the neural circuits do not develop, resulting in amblyopia<sup>2,3</sup>. Processing visual information in early childhood promotes the formation of synapses in the brain, while efficiently pruning unnecessary synapses enhances an individual's ability to process visual information in the future<sup>4</sup>. Patients who lost sight during childhood and were treated with visual regeneration therapy in adulthood were reportedly able to perceive light but not visual information, whereas those who lost sight during adulthood and were treated later recovered their vision<sup>2,3</sup>. These findings indicate that visual experiences in childhood are important for the construction of visual information processing mechanisms and that the critical period is an important time for building brain function.

Functional magnetic resonance imaging (fMRI) of the brain recently demonstrated that patients who lose vision in childhood have a more activated visual cortex in response to sound than those with clear vision<sup>5</sup>; such changes in brain function have been attributed to brain plasticity. Early blindness is believed to cause expansion of the auditory cortex because the visual cortex no longer processes visual information. Piche et al.<sup>6</sup> also reported that the primary visual cortex responded to auditory stimulation in a rat model of blindness, suggesting cross-modal compensation in blind individuals. However, it is not fully understood which areas of the visual cortex represent the initial auditory response.

<sup>1</sup>Laboratory of Visual Neuroscience, Graduate Course in Biological Sciences, Iwate University Division of Science and Engineering, 4-3-5 Ueda, Morioka Iwate 020-8551, Japan. <sup>2</sup>KDDI Research, Inc, 2-1-15 Ohara, Fujimino Saitama 356-8502, Japan. <sup>3</sup>Faculty of Science and Engineering, Shokei Gakuin University, 4-10-4 Yurigaoka, Natori, Miyagi 981-1295, Japan. <sup>4</sup>Graduate Course in Biological Sciences, Division of Science and Engineering, Iwate University, 4-3-5 Ueda, Morioka Iwate 020-8551, Japan. <sup>5</sup>Shu Maruoka and Eriko Sugano contributed equally to this work. ✉email: htomita@iwate-u.ac.jp

We previously used intrinsic optical signal (IOS) imaging to visualise the responses in the visual cortex to light and sound stimulation<sup>7,8</sup>. IOS imaging is based on neurovascular coupling<sup>9</sup> as follows: following neural cell excitation, the  $\text{Ca}^{2+}$  concentration in brain neurones increases, the vascular smooth muscle and endothelium relax, and the local cerebral blood volume around the excited region increases. Because haemoglobin strongly absorbs green light, the spatiotemporal activity of the local blood volume can be measured by irradiating the cerebral cortex with green light of a certain intensity and observing the scattered light. Thus, IOS imaging does not require special equipment, such as MRI, to investigate brain activity<sup>10,11</sup>.

Here we report audiovisual plasticity at the cortical level following blindness in Royal College of Surgeons (RCS) rats<sup>12,13</sup>. Electrophysiological studies revealed that the visual cortex underwent photoreceptor degeneration, which rapidly and significantly increased auditory responses compared to normal rats continued until 7 months of age. The entire visual cortex of blind rats responded to white-noise stimuli, whereas only the ventral side of the visual cortex responded in normal rats. Thus, here we demonstrated the local characteristics of the visual cortex in response to sound stimuli caused by brain plasticity following blindness.

## Results

### Photoreceptor degeneration

An optical coherence tomography (OCT) image of 3-month-old wild-type RCS (+/+) rats demonstrated a normal retinal architecture (Fig. 1A), whereas a loss of photoreceptor cells was observed in 3-month-old RCS rats (rdy/rdy) (Fig. 1B). The thickness of the retinal layer was significantly ( $p < 0.001$ ) reduced in 3-month-old RCS rats (rdy/rdy) (Fig. 1C). Retinal function was assessed using scotopic electroretinography (ERG) recording. There were no detectable a- and b-waves in 3-month-old RCS (rdy/rdy) rats (Fig. 1D). The a-wave is an early negative wave (downward wave) of the ERG waveform that indicates the photoreceptor cell response to light stimuli. The b-wave is a positive wave (upward wave) produced by Müller and bipolar cells within the retina.

### Visual cortex responses by light or sound stimulation

Visual cortex responses (VCRs) with light stimuli, generally known as visually evoked potentials, were observed in normal RCS (+/+) rats (Fig. 2A) but not in 3-month-old photoreceptor-degenerated RCS (rdy/rdy) rats (Fig. 2B). VCRs to white-noise stimuli (all frequency components were equally contained) were recorded in 3-month-old rats (Fig. 2C and D). Significant differences were observed in the N1–P1 amplitudes between normal and blind rats (Fig. 2E), and the largest response was observed in 4 month-old rats. These differences persisted up to 7 months of age (Fig. 2F).

### IOS imaging of normal versus blind rats

The recording condition of the IOS imaging is shown in Fig. 3 A and B. The cortex surface image during the recordings is presented in Fig. 3C, corresponding to the visual cortex as shown by a photograph of a transcranial observation (Fig. 3D). IOS imaging with visual stimuli in RCS (+/+) rats ( $n = 3$ ) demonstrated reflectance variability throughout the visual cortex (Fig. 3 E and F). In addition, RCS (+/+) rats elicited a local response in the right visual cortex (Fig. 3G) when RCS (+/+) rats were stimulated in the left eye only. On the other hand, RCS (rdy/rdy) rats ( $n = 4$ ) showed no reflectance variability (Fig. 3H and I), and no response was also elicited in the right visual cortex when RCS (rdy/rdy) rats were stimulated in the left eye only (Fig. 3J). Both RCS (+/+) (Fig. 4A and B) and RCS (rdy/rdy) rats (Fig. 4C and D) showed an IOS corresponding to the sound stimulus; however, the RCS (rdy/rdy) rats showed a higher IOS than the RCS (+/+) rats.

## Discussion

RCS rats are used as an animal model of recessively inherited photoreceptor degeneration by dysfunction of phagocytosis in the retinal pigment epithelium<sup>14</sup> that results in a progressive postnatal loss of photoreceptor cells. Retinal development normally occurs in RCS rats; however, functional changes on ERG appear at 1 month of age<sup>15</sup>, and the loss of photoreceptor cells is complete by 3 months of age. Thus, RCS rats, which develop a normal visual system but gradually become blind, are a good model for investigating visual cortex plasticity.

The OCT (Fig. 1B) and ERG (Fig. 1D) results indicated that visual input from the eye to the visual cortex was expected to be ineffective in 3-month-old RCS (rdy/rdy) rats. Defects in sensory input are known to lead to the remodelling of neuronal architecture<sup>16,17</sup>.

Indeed, VCR amplitudes in response to sound but not light stimuli were larger in RCS (rdy/rdy) rats than in RCS (+/+) rats (Fig. 2C and D). Importantly, RCS (+/+) rats exhibited a general response to VCRs with light stimuli, whereas RCS rdy/rdy rats showed no response. These results indicate that RCS (rdy/rdy) rats had no neural input from light to the visual cortex. Nevertheless, VCRs to sound stimuli were significantly higher in RCS (rdy/rdy) rats than in RCS (+/+) rats. VCRs with sound stimuli were also recorded in RCS (+/+) rats because they are nocturnal animals and more dependent on their auditory and tactile senses than on their vision. Hirokawa et al. reported that the visual area in rats is involved in multisensory facilitation induced by a combination of auditory and visual stimuli<sup>18</sup>, which may have originally used the visual cortex to process the perception of the environment through sound<sup>18–20</sup>. In many animals including humans, the visual cortex can perform echolocation (bioacoustic technology used by organisms to detect the surrounding environment using sound waves and discern the position and shape of objects), during which hyperactivity of the visual cortex can be observed<sup>5,21,22</sup>.

Loss of visual input to the visual cortex due to photoreceptor degeneration in the retina reportedly enhances the auditory response in the visual cortex (Fig. 2D). Peak enhancement occurred at 4 months, which almost coincided with the onset of photoreceptor degeneration. After 4 months, the increased auditory response in the visual cortex declined, and significant enhancement was observed until 8 months of age (Fig. 2F). However, no

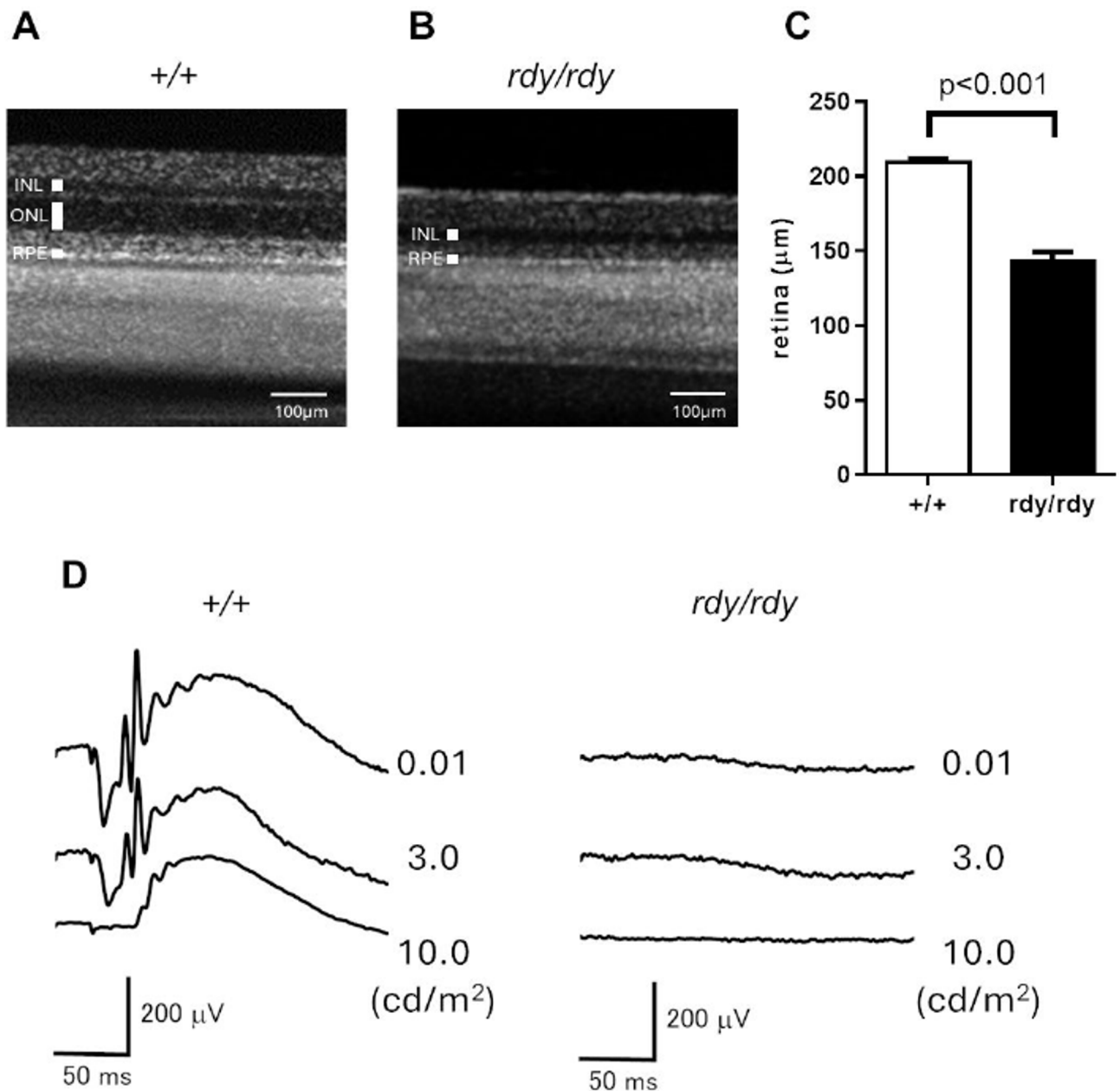


**Fig. 1.** Comparisons of retinal structures and functions in Royal College of Surgeons (RCS) ( $+/+$ ) and RCS ( $rdy/rdy$ ) rats. Representative optical coherence tomography images of an RCS ( $+/+$ ) rat (A) and an RCS ( $rdy/rdy$ ) rat (B) are shown. Comparison of whole retinal thickness (C). The data are presented as mean  $\pm$  standard error ( $+/+$ :  $n=4$ ;  $rdy/rdy$ :  $n=10$ ; Student's  $t$ -test,  $***p < 0.001$ ). Representative electroretinography waveforms were recorded at stimuli of 0.01, 3.0, and 10.0  $\text{cd}/\text{m}^2$  from an RCS ( $+/+$ ) rat and an RCS ( $rdy/rdy$ ) rat (D). INL, inner nuclear layer; ONL, outer nuclear layer; RPE, retinal pigment epithelium.

significant change was seen before 8 months, the end of the critical phase of the visual cortex. The mechanism by which an increased auditory response decreases is unclear; however, auditory sensitivity might transiently increase with the timing of blindness due to neuroplasticity, after which point the blind rats would gradually adapt to their environment using sound only, while their auditory enhancement would decrease. However, further studies are needed to confirm this hypothesis.

The results of IOS imaging indicated that the role of the visual cortex was replaced by auditory function after visual function loss and that the visual cortex became highly responsive to sound stimuli due to blindness. The heatmap of the visual stimuli of normal rats and audio stimuli of blind rats (Figs. 3E and 4D) showed that the high-response area was along the sagittal suture. These results strongly support the idea that the primary visual cortex provides an auditory function upon visual ability loss. Normal rats appeared to have synaesthesia of the visual and auditory senses as previously reported. Functional changes in the visual cortex were caused by a lack of visual ability due to early blindness<sup>23</sup>.

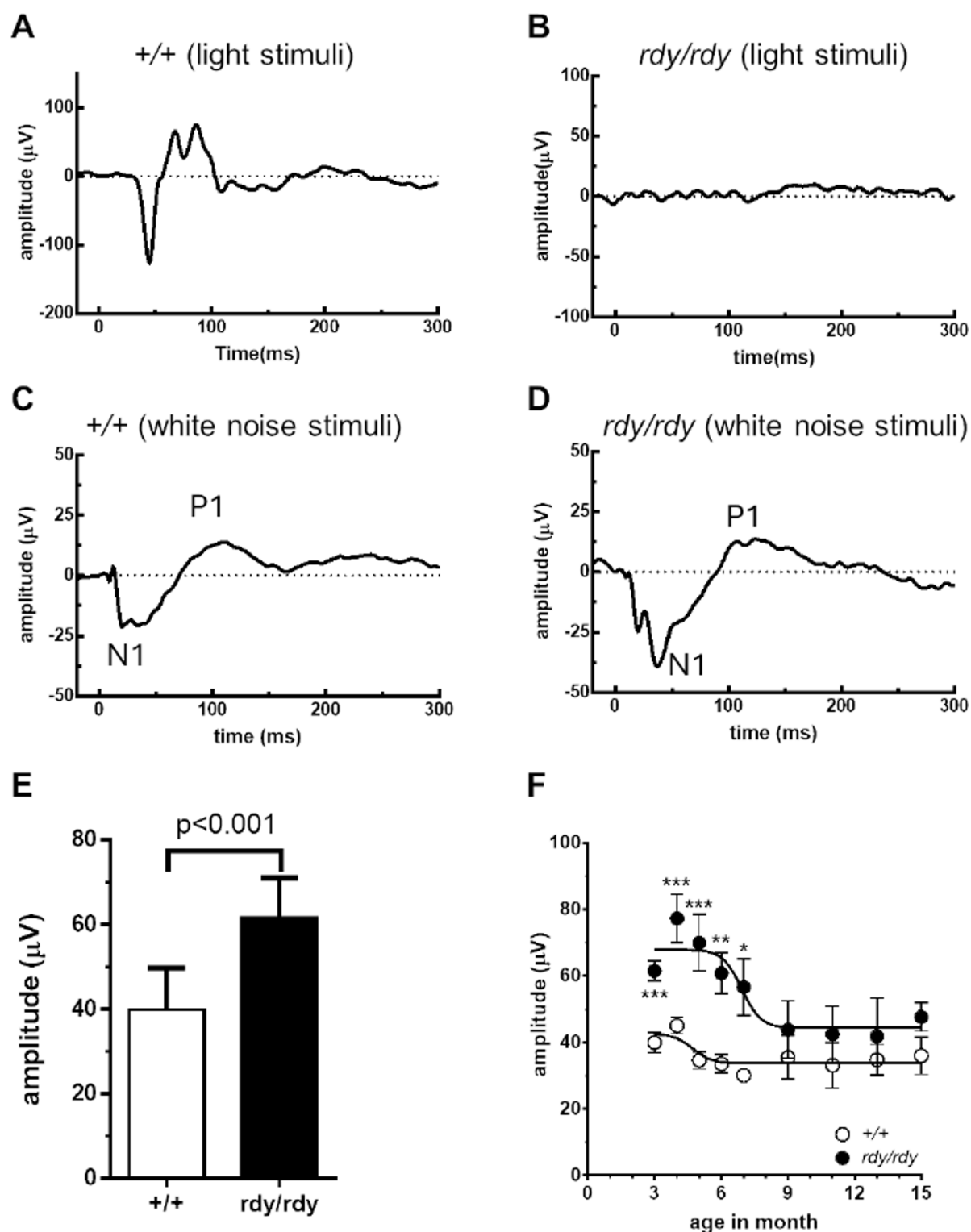


**Fig. 2.** Recordings of the visual cortex response (VCR) to light or white-noise stimuli. Typical waveforms of VCRs with light (A, B) or white-noise (C, D) stimuli in Royal College of Surgeons (RCS) (+/+) and RCS (rdy/rdy) rats. Amplitudes (N1–P1) evoked from white-noise stimuli were significantly increased in the 3-month-old photoreceptor-degenerated RCS (rdy/rdy) rats. The data are presented as mean  $\pm$  standard error (+/+;  $n = 10$ ; rdy/rdy:  $n = 10$ ). The data were analysed using an unpaired t-test ( $***p < 0.001$ ). (E,F) Changes in audio-VCR amplitudes over time in RCS (+/+) and RCS (rdy/rdy) rats. The data are presented as mean  $\pm$  standard error (+/+;  $n = 4$ ; rdy/rdy:  $n = 10$ ; Student's t-test,  $***p < 0.001$ ). Representative electroretinography waveforms were recorded at 0.01, 3.0, and 10.0  $\text{cd/m}^2$  (D) stimuli.

C-Fos staining is often used to assess responsive regions of the cortex. The expression of c-Fos, a marker of neural activity, in tinnitus-induced gerbils was confirmed in both the auditory and non-auditory regions of the brain<sup>24</sup>. Moreover, c-Fos is expressed in the amygdala<sup>25,26</sup> in response to acute stress. It is difficult to determine whether c-Fos expression is induced by stress or as a response to stimuli. Therefore, the present study focused on IOS imaging. IOS imaging, based on blood volume, is a unique method for identifying local areas that respond to stimuli. We determined that the IOS were suitable for local responses because we stimulated only the left eye of normal and blind rats and demonstrated a local response in the right brain of normal rats versus no response in blind rats (Fig. 3E and H). The area in response to visual stimuli in RCS (+/+) rats (Fig. 3E) resembled that in response to sound stimuli in blind RCS (rdy/rdy) rats (Fig. 4D). These results also suggested that the echolocation used by the blind rats originated from the primary visual cortex.

The human primary visual cortex can be used for echolocation, as shown by fMRI studies, which demonstrated that auditory mapping in the primary visual cortex correlates with visual mapping in visually normal subjects, whereas no correlation was demonstrated in visually impaired individuals who are unable to perform echolocation<sup>27</sup>. The fact that auditory responses in the primary visual cortex were detected of blind and normal rats but the response area size and magnitude were larger from the former suggests that early blindness accelerates cross-modal plasticity. However, the mechanisms underlying accelerated plasticity in blind rats remain unclear.

Experience-dependent synaptic modifications in the striate cortex are reportedly disrupted by an *N*-methyl-D-aspartate (NMDA) receptor antagonist infusion<sup>28,29</sup>. Further studies using an NMDA receptor antagonist might be useful for elucidating the mechanism underlying plasticity, and IOS imaging would contribute to the identification of areas of plasticity.

## Methods

### Animals

All rats were housed under conditions of cyclic light (on at 8:00 a.m., 5 lx; off at 8:00 p.m., 0 lx) at  $23 \pm 1$  °C. The rats had free access to water. All of the animal experiments were performed in accordance with the Association for Research in Vision and Ophthalmology statement for the Use of Animals in Ophthalmic and Vision Research, the Guidelines of the Iwate University Animal Experimentation Committee on Animals in Research, and the ARRIVE guidelines (<https://arriveguidelines.org>). RCS (rdy/rdy,  $n = 10$ ) and wild-type RCS (+/+,  $n = 4$ ) rats were obtained from CLEA Japan Inc. (Tokyo, Japan)<sup>12,30,31</sup>. Wild-type RCS rats with a normal retinal architecture and function were used as controls.

### OCT imaging

OCT imaging was performed as previously described<sup>32</sup>. Briefly, the rats were anaesthetised with an intramuscular injection of ketamine (75 mg/kg) and medetomidine (0.5 mg/kg), and their pupils were dilated with tropicamide (Midrin-P, Santen Co., Ltd., Osaka, Japan). Each eye was anesthetized using oxybuprocaine (Santen Co., Ltd., Osaka, Japan) and covered with a contact lens. Images of the rat retina (1.1-mm long including the optic disc) were acquired using the line scan mode on an OCT imaging device equipped with a specially ordered lens (RS-3000; NIDEK Co., Ltd., Aichi, Japan).

### ERG and VCR recordings

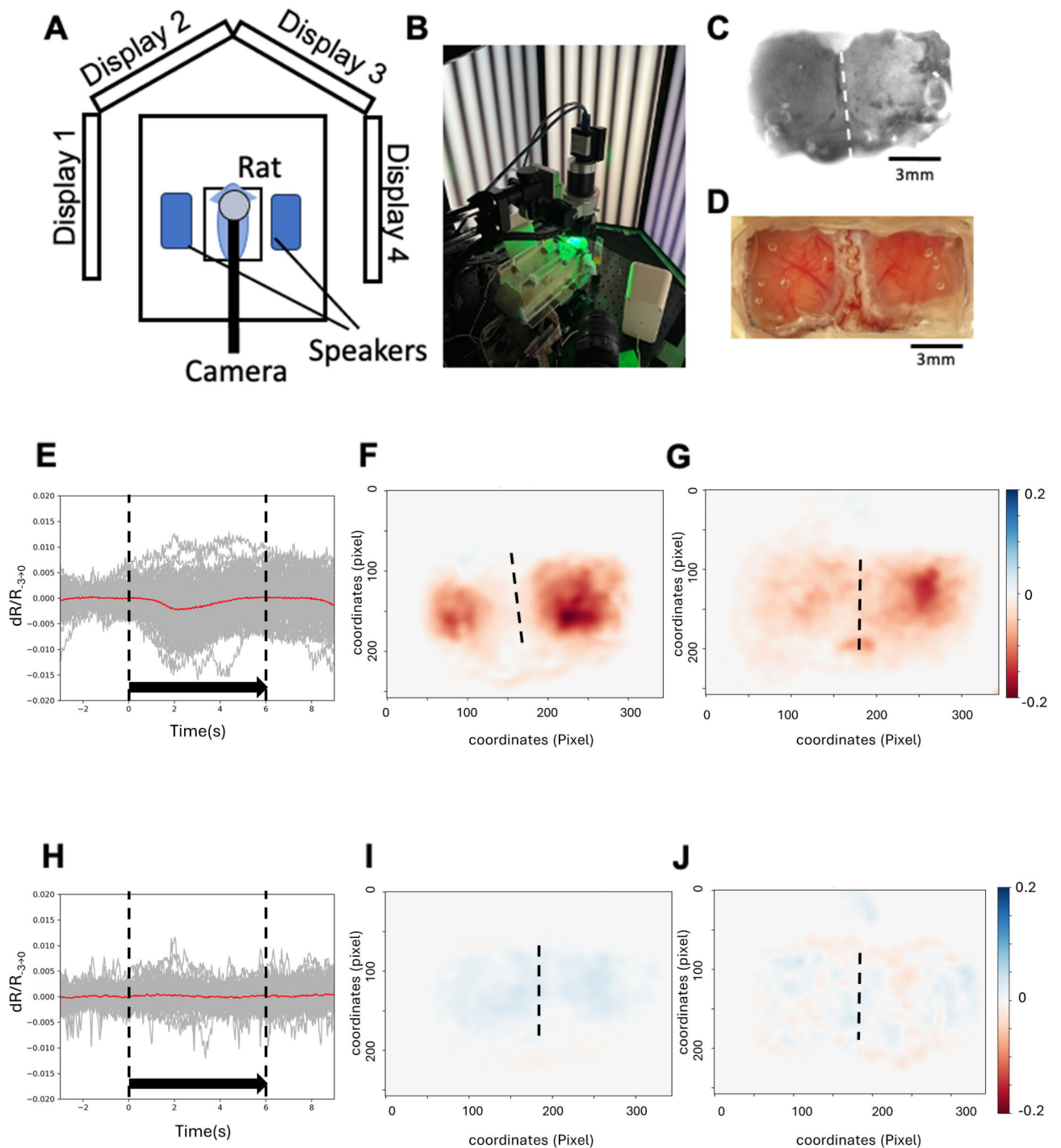
ERG and VCR recordings were made using a PuREC system (Mayo, Inazawa, Japan) as previously described with slight modifications. For the ERG recordings, the rats were dark-adapted overnight. Under ketamine-medetomidine anaesthesia, their pupils were dilated with 0.5% tropicamide and 0.5% phenylephrine hydrochloride. A small contact lens with an electrode was mounted on the cornea and a reference electrode was placed in the oral cavity. Photic stimuli were generated using white light-emitting diodes (LEDs). The photic stimuli were applied for 5 ms. The high- and low-pass filters were set at 1 kHz and 0.5 Hz, respectively.

For VCRs of light or auditory stimulation, recording electrodes (stainless screws) were embedded epidurally on each side (6.8 mm behind the bregma, 3 mm lateral to the midline), and a reference electrode (a stainless screw) was embedded epidurally on the midline at 11.8 mm behind the bregma at least 7 days before the experiments. The VCRs were recorded by setting the high- and low-pass filters to 50 Hz and 0.05 Hz, respectively. Light or sound stimuli were applied at a frequency of 1 Hz for 10 ms. Each VCR was consecutively recorded 200 times, and response waveforms were averaged for each measurement.

VCRs induced by light stimulation are generally referred to as visually evoked potentials. The rat eyes were subjected to photic stimuli using blue LEDs (468 nm, 80.7  $\mu$ W/mm<sup>2</sup>). In the sound stimuli experiments, white noise (70 dB, 0.02–4 kHz) produced by a speaker (0.5 W, 8  $\Omega$ ; Uxcell, Japan) was used for the auditory stimulation.

### IOS imaging

Preparation of rats: Surgery was performed on the rats 1–3 weeks before the IOS imaging. Under isoflurane anaesthesia, the skull was partially exposed by removal of part of the rat's scalp and thinly shaved such that the surface of the brain could be observed transcranially, and a cover glass was glued over the thinly shaved area with clear dental cement (Sum Medical Co., Shiga, Japan). The area corresponding to the visual cortex was visualised transcranially. A head-fixation plate was glued to the skull to painlessly fix the head to the holding box. The surgical area was the visual cortex (V1). We targeted V1 for the IOS recordings so the surgery was performed 4 mm behind the bregma, 3 mm ahead of the lambda, and 6 mm left or right of the sagittal suture. Postoperatively, all rats were raised individually, and no health hazards or behavioural changes due to the surgery were observed.



#### Recording conditions

A light-emitting diode ( $525 \text{ nm} \pm 10 \text{ nm}$ ; Prizmatix Ltd., Holon, Israel) was transcranially projected onto the cerebral cortex of the rat in a dark room, and the scattered light reflected from the surface of the cerebral cortex while the rat was watching moving stripes presented on the display (LCD-MF277XDB; I-O Date Device Inc., Ishikawa, Japan) or auditory white noise was recorded. Screen brightness for visual stimuli was  $300 \text{ cd/m}^2$ . In this experiment, we focused on changes in the total volume of blood in the visual cortex. We used green light because the haemoglobin absorption of green light was high, and oxygenated and deoxygenated blood samples were not measured separately<sup>33</sup>. Surface images of the visual cortex during stimulation were captured using FlyCapture 2 software (FLIR Systems, Inc., Wilsonville, OR). A fluorescence microscope (housing, custom, N & N; objective lens, XLFLUOR4X/340; NA = 0.28; Olympus, Inc., Tokyo, Japan) equipped with a cooled charge-coupled device camera (ORCA-R2; Hamamatsu Photonics K.K., Shizuoka, Japan) was used to acquire the images.

#### Visual stimuli

Striped patterns as the visual stimuli were placed around the rat at  $240^\circ$  horizontal ( $120^\circ$  left,  $120^\circ$  right) and  $85.5^\circ$  of elevation ( $27.3^\circ$  downward,  $57.2^\circ$  upward) from the liquid crystal display. The stimulus conditions were

**Fig. 3.** Intrinsic optical signal imaging of the visual cortex from visual stimuli. Experimental diagram (A). Four displays for producing visual stimuli were placed around the rat, and a speaker for auditory stimuli was set at each ear. The rat was fixed in a holding box, and a camera acquiring images of the surface of the visual cortex was placed above its head. A view of the visual stimulus experiment (B). Example of cortex surface image used in this experiment (C). The white-dashed line shows the sagittal suture. This area is 6–9 mm behind the bregma and 6 mm left or right from the sagittal suture. A photograph of a transcranial observation of the visual cortex after surgery (D). Visual stimulation formed sine-waved stripes presented on four displays covering the entire field of view. Averaged waveform (red line) calculated from all trials (grey lines) stimulating a full field of view in a Royal College of Surgery (RCS) (+/+) rat and an RCS (rdy/rdy) rat are shown in (E) and (H), respectively. In (E) and (H), the vertical and horizontal axes indicate the changes in green-reflected light and the time course, respectively. The black arrow indicates the visual stimulus. Typical response area map of the visual cortex stimulating a full field of view in an RCS (+/+) rat (F) and an RCS (rdy/rdy) rat (I). Typical response area map of the visual cortex stimulating only the left eye in an RCS (+/+) rat (G) and an RCS (rdy/rdy) rat (J). The black-dashed lines in the heatmap (F, H, I, and J) indicate the sagittal suture in each image. All data analyses were performed using Python. X and Y mean coordinates of the pixel (1 pixel = 0.04 mm). The vertical axis of (F) and (G) and the units of the coloured bars in (I) and (J) are %. The heatmaps were made of reflectance changes from a visual cortex during stimulation.

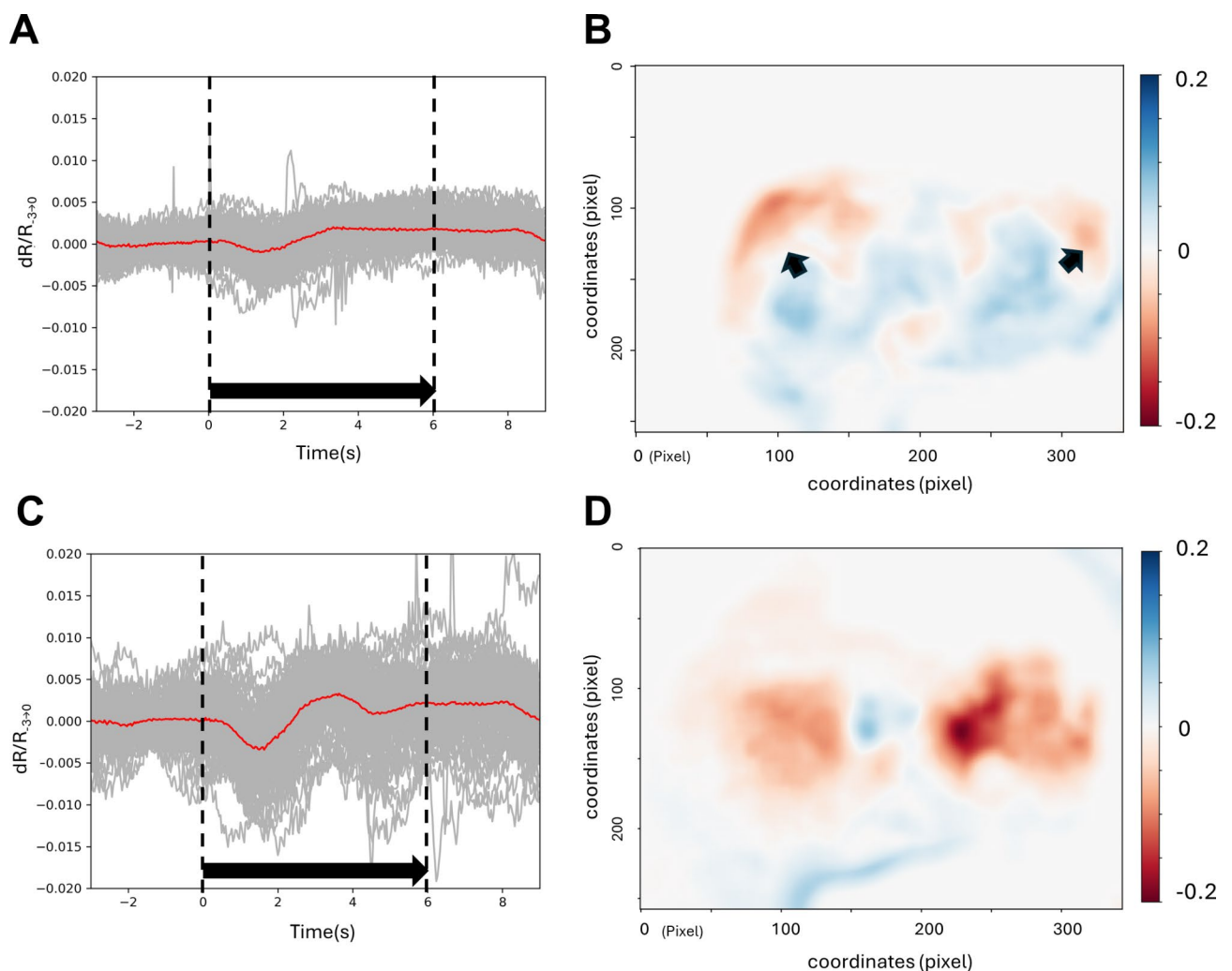


**Fig. 4.** Intrinsic optical signal imaging of the visual cortex from white noise stimuli. Averaged waveform (red line) calculated from all trials (grey lines) stimulating white noise in a Royal College of Surgery (RCS) (+/+) rat (A) and an RCS (rdy/rdy) rat (C). Typical response area map of the visual cortex stimulated by white noise in an RCS (+/+) rat (B) and an RCS (rdy/rdy) rat (D). The black arrow in (B) shows the responsive region. The dashed black lines in the heatmap shown in (B) and (D) represent the sagittal suture in each image. The vertical axis shown in (A) and (C) and the units of the coloured bar shown (B) and (D) are %.

random stripes in the left and right directions at a spatial frequency of 0.0625–0.5 cycles/degree and a rotation speed of 0.75–96 rpm, respectively. The stimulus cycle was repeated 96 times.

#### Auditory stimuli

White noise excluding 60–20,000 Hz (no frequency response) at an intensity of 70 dB for 6 s with a stimulus interval of 6 s was used as the auditory stimulus. The stimulus cycle was repeated 100 times. All heat maps were created using the average reflectance of the stimuli.

#### Statistical analysis

The statistical analyses were performed using GraphPad Prism 4 software (GraphPad, San Diego, CA, USA). The statistical methods used were an unpaired t-test and Dunnett's multiple comparison test.

#### Data availability

The datasets used and/or analysed in the current study are available from the corresponding author upon reasonable request.

Received: 25 June 2024; Accepted: 11 October 2024

Published online: 05 November 2024

#### References

- Levelt, C. N. & Hübner, M. Critical-period plasticity in the visual cortex. *Annu. Rev. Neurosci.* **35**, 309–330 (2012).
- Huber, E. et al. A lack of experience-dependent plasticity after more than a decade of recovered sight. *Psychol. Sci.* **26**, 393–401 (2015).
- Kalia, A. et al. Development of pattern vision following early and extended blindness. *Proc. Natl. Acad. Sci. U S A.* **111**, 2035–2039 (2014).
- Faust, T. E., Gunner, G. & Schafer, D. P. Mechanisms governing activity-dependent synaptic pruning in the developing mammalian CNS. *Nat. Rev. Neurosci.* **22**, 657–673 (2021).
- Thaler, L., Arnott, S. R. & Goodale, M. A. Neural correlates of natural human echolocation in early and late blind echolocation experts. *PLoS One.* **6**, e20162 (2011).
- Piche, M. et al. Auditory responses in the visual cortex of neonatally enucleated rats. *Neuroscience.* **145**, 1144–1156 (2007).
- Haglund, M. M. & Hochman, D. W. Imaging of intrinsic optical signals in primate cortex during epileptiform activity. *Epilepsia.* **48** (Suppl 4), 65–74 (2007).
- Hillman, E. M. C. Optical brain imaging in vivo: techniques and applications from animal to man. *J. Biomed. Opt.* **12**, 051402 (2007).
- Attwell, D. et al. Glial and neuronal control of brain blood flow. *Nature.* **468**, 232–243 (2010).
- Kalatsky, V. A. & Stryker, M. P. New paradigm for optical imaging: temporally encoded maps of intrinsic signal. *Neuron.* **38**, 529–545 (2003).
- Schuett, S., Bonhoeffer, T. & Hübner, M. Mapping Retinotopic structure in Mouse Visual Cortex with optical imaging. (2002).
- LaVail, M. M. & Battelle, B. A. Influence of eye pigmentation and light deprivation on inherited retinal dystrophy in the rat. *Exp. Eye Res.* **21**, 167–192 (1975).
- Wiesel, T. N. & Hubel, D. H. SINGLE-CELL RESPONSES IN STRIATE CORTEX OF KITTENS DEPRIVED OF VISION IN ONE EYE.
- Bok, D. & Hall, M. O. The role of the pigment epithelium in the etiology of inherited retinal dystrophy in the rat. *J. Cell. Biol.* **49**, 664–682 (1971).
- Dowling, J. E. & Sidman, R. L. Inherited retinal dystrophy in the rat. *J. Cell. Biol.* **14**, 73–109 (1962).
- Maya Vetencourt, J. F. et al. The antidepressant fluoxetine restores plasticity in the adult visual cortex. *Sci.* (1979). **320**, 385–388 (2008).
- Guirado, R. et al. Effects of PSA removal from NCAM on the critical period plasticity triggered by the antidepressant fluoxetine in the visual cortex. *Front. Cell. Neurosci.* **10**, 22 (2016).
- Hirokawa, J., Bosch, M., Sakata, S., Sakurai, Y. & Yamamori, T. Functional role of the secondary visual cortex in multisensory facilitation in rats. *Neuroscience.* **153**, 1402–1417 (2008).
- Rosenzweig, M. R., Riley, D. A. & Krech, D. Evidence for echolocation in the rat. *Sci.* (1979). **121**, 600 (1955).
- Echolocation in the Blinded Rat EXPERIMENT 1 Method.* (1971).
- Thaler, L. & Foresteire, D. Visual sensory stimulation interferes with people's ability to echolocate object size. *Sci. Rep.* **7**, 13069 (2017).
- Brainard, M. S. & Knudsen, E. I. Sensitive periods for visual calibration of the auditory space map in the barn owl optic tectum. *J. Neurosci.* **18**, 3929–3942 (1998).
- Deneux, T. et al. Context-dependent signaling of coincident auditory and visual events in primary visual cortex. doi: (2019). <https://doi.org/10.7554/eLife.44006.001>
- Wallhauser-Franke, E. et al. Expression of c-fos in auditory and non-auditory brain regions of the gerbil after manipulations that induce tinnitus. *Exp. Brain Res.* **153**, 649–654 (2003).
- Kang, J. W. M., Mor, D. & Keay, K. A. Nerve injury alters restraint-induced activation of the basolateral amygdala in male rats. *Brain Struct. Funct.* **226**, 1209–1227 (2021).
- Ceccatelli, S., Villar, M. J., Goldstein, M. & Hokfelt, T. Expression of c-Fos immunoreactivity in transmitter-characterized neurons after stress. *Proc. Natl. Acad. Sci. U S A.* **86**, 9569–9573 (1989).
- Norman, L. J. & Thaler, L. Retinotopic-like maps of spatial sound in primary 'visual' cortex of blind human echolocators. *Proc. Biol. Sci.* **286**, 20191910 (2019).
- Bear, M., Kleinschmidt, A., Gu, Q. & Singer, W. Disruption of experience-dependent synaptic modifications in striate cortex by infusion of an NMDA receptor antagonist. *J. Neurosci.* **10**, 909–925 (1990).
- Kleinschmidt, A., Bear, M. F. & Singer, W. Blockade of 'NMDA' receptors disrupts experience-dependent plasticity of Kitten Striate Cortex. *Science.* **238**, 355–358 (1979). 1987.
- D'Cruz, P. M. et al. Mutation of the receptor tyrosine kinase gene MERTK in the retinal dystrophic RCS rat. *Hum. Mol. Genet.* **9**, 645–651 (2000).
- Tomita, H. et al. Restoration of visual response in aged dystrophic RCS rats using AAV-mediated channelopsin-2 gene transfer. *Invest. Ophthalmol. Vis. Sci.* **48**, 3821–3826 (2007).
- Sato, M. et al. Visual responses of photoreceptor-degenerated rats expressing two different types of channelrhodopsin genes. *Sci. Rep.* **7**, 41210 (2017).

33. Tromberg, B. J. *et al.* Non-Invasive In Vivo Characterization of Breast Tumors Using Photon Migration Spectroscopy I. [www.nature.com/neo](http://www.nature.com/neo)

## Acknowledgements

We express our heartfelt appreciation to Yoko Takahashi and Miho Sato of the Laboratory of Visual Neuroscience for preparing the histological sections and maintaining the experimental equipment used in this study.

## Author contributions

S.M. performed the IOS imaging. E.S. supervised the experiments. R.T. and N.K. analysed the IOS imaging data. K.T. performed the electrophysiological recordings. N.Y. and R.M. performed the IOS imaging. Y.T., T.O., T.F., and L.B. provided critical suggestions. H.T. designed the experiments and wrote the manuscript.

## Funding

This research was funded by Grants-in-Aid for Scientific Research from the Ministry of Education, Culture, Sports, Science, and Technology in Japan (grant nos. 22H00579, 21K18278, 22K09760, 21K09713, and JP22H04922 [AdAMS] and TERUMO LIFE SCIENCE FOUNDATION [21-II4001]).

## Declarations

## Competing interests

The authors declare no competing interests.

## Additional information

**Correspondence** and requests for materials should be addressed to H.T.

**Reprints and permissions information** is available at [www.nature.com/reprints](http://www.nature.com/reprints).

**Publisher's note** Springer Nature remains neutral with regard to jurisdictional claims in published maps and institutional affiliations.

**Open Access** This article is licensed under a Creative Commons Attribution-NonCommercial-NoDerivatives 4.0 International License, which permits any non-commercial use, sharing, distribution and reproduction in any medium or format, as long as you give appropriate credit to the original author(s) and the source, provide a link to the Creative Commons licence, and indicate if you modified the licensed material. You do not have permission under this licence to share adapted material derived from this article or parts of it. The images or other third party material in this article are included in the article's Creative Commons licence, unless indicated otherwise in a credit line to the material. If material is not included in the article's Creative Commons licence and your intended use is not permitted by statutory regulation or exceeds the permitted use, you will need to obtain permission directly from the copyright holder. To view a copy of this licence, visit <http://creativecommons.org/licenses/by-nc-nd/4.0/>.

© The Author(s) 2024